Paper
Int'l J. of Aeronautical & Space Sci. 15(1), 102–111 (2014)
DOI:10.5139/IJASS.2014.15.1.102

IJASS
International Journal of Aeronautical and Space Sciences

Performance Modeling of a Pyrotechnically Actuated Pin Puller

Seung-gyo Jang*, Hyo-nam Lee and Jong-yun Oh*****

Advanced Propulsion Technology Center, Agency for Defense Development, Yuseong P.O. Box 35, Daejeon 305-600, Republic of Korea

Abstract

An analytical model was developed to understand the physics and predict the functional performance of a pin puller. The formulated model is based on one-dimensional gas dynamics for an ideal gas. Resistive forces against pin shaft movement were measured in quasi-static mechanical tests, the results of which were incorporated into the model. The expansion chamber pressure and the pin shaft displacement were measured from an actual firing test and compared to the model prediction. The gas generation rate was adjusted by a correction factor, and the heat transfer rate was obtained through parametric analysis. The validity of the model is assessed for additional firing tests with different amounts of pyrotechnic charge. This model can provide knowledge on how the pin puller functions, and on which design parameters contribute the most to the actuation of the pin puller. Using this model, we estimate the functional safety factor by comparing the energy generated by the pyrotechnic charge to the energy required to accomplish the function.

Key words: Pin Puller, Pyrotechnic Actuator, Initiator, Safety Factor

1. Introduction

A pin puller is one of the cartridge-actuated-devices (CADs) that are widely used in military and aerospace applications [1]. Figure 1 shows a schematic of a newly developed pin puller for releasing a missile from a launch tube. The pin puller consists of a pyrotechnic initiator, a pin shaft, housing, and locking mechanism. The initiator, usually mounted on the housing by a thread, contains the pyrotechnic charge and bridge-wires. The shear pin is used initially to hold the pin shaft in place, and the O-rings fitted on the pin shaft are used to prevent the combustion gases from leaking.

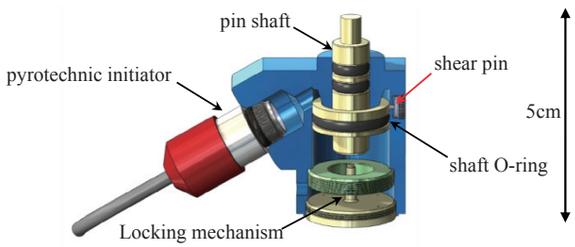

Fig. 1. Pyrotechnically actuated pin puller

As a firing current is applied to the bridge-wires, the burning pyrotechnic charge pressurizes the expansion chamber of the housing. High pressurized gases exert a force on the pin shaft, resulting in cutting off the shear pin and accelerating the pin shaft downward to the bottom of the housing. If the generated force is sufficient to overcome the resistive forces against pin shaft movement, it can be retracted into the intended stroke. The retraction to the predetermined stroke results in missile release.

Generally, due to the excessive energy of the moving pin shaft, various energy absorption mechanisms are employed near the end of the stroke to reduce the pyrotechnic shock and to prevent rebound of the pin shaft. In the present study, a particular energy absorption mechanism was devised called the "locking mechanism". The locking mechanism prevents the pin shaft from bouncing after reaching the full stroke. The locking is achieved by plastic deformation caused by dimensional interference between the stud of the housing

* Corresponding author: jsg4580@add.re.kr
** Principal Researcher: lhn4577@add.re.kr
*** Principal Researcher: jyo4526@add.re.kr

Received: December 19, 2013 Revised : February 4, 2014 Accepted: March 4, 2014

http://ijass.org pISSN: 2093-274x eISSN: 2093-2480

and bore of the pin shaft; that is, the diameter of the stud is slightly larger than that of the bore (see Fig. 2 for details). As the moving distance of the pin shaft increases to a near full stroke, the pin shaft is eventually anchored due to the energy dissipation by plastic deformation. In this respect, the locking mechanism is a special energy absorbing system that converts the kinetic energy of the moving pin shaft into plastic deformation energy.

For the pin puller of the present study, the housing and pin shaft are both made of stainless steel, 17-4pH. The pin shaft mass m_p is 0.0144 kg. The initial internal volume of the expansion chamber V_o is 650 mm^3, and the full stroke of the pin shaft is 9.2 mm. The shear pin is made of 6061-T6 aluminum with a diameter of 0.8 mm. The stud at the locking mechanism is made of STS 304. The pyrotechnic initiator contains 53 mg of $ZrKClO_4$ (Zirconium Potassium Per-chlorate (ZPP)) powder pressed onto the bridge-wires. A stainless steel closure disk is welded at the end of the charge column in the initiator to guarantee a hermetic seal.

Usually, CADs are used where mission-critical function is needed. For example, failure of the pin puller can lead to missile launch failure. Therefore, very high reliability is necessary, and reliability evaluation is very important for both estimation and demonstration. According to the traditional reliability method, reliability can be evaluated using failure data obtained from a large number of functional tests. In the case of the CADs, however, reliability evaluation is not easy in reality due to their 'one-shot' nature; CADs cannot be used after being fired because the firing test is accompanied by irreversible processes such as burning of the pyrotechnic charge and destruction of components. Due to this destructive nature, the pin puller cannot be tested repeatedly for reliability evaluation, unlike other mechanical

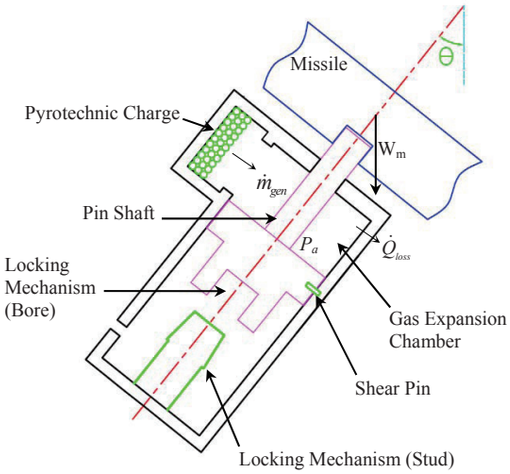

Fig. 2. Illustration of pin puller subsystem

or electronic systems. Eventually, available failure data for reliability evaluation are limited in terms of cost and time. In this respect, evaluating the reliability of such one-shot devices has become a troublesome challenge.

The traditional reliability methods [2-5] have another shortcoming, since they depend on a large number of actual firings. Firing tests do not give the information needed to understand the functional performance of the device. Nonetheless, they are necessary to observe actual device behavior. A lack of understanding about the functional performance can lead to catastrophic failures when the device is applied to unexpected conditions. This means that the physics of the device should be understood to reduce the failure probability and to improve the design.

For this reason, computational modeling approaches can be helpful. Over the last two decades, a great deal of research has been carried out on computational modeling related to the performance of several types of CAD [6-14]. These works provide information on the CAD system physics, which enables designers to predict and analyze the performance of devices. Most of the works, however, have focused merely on the calculation of the combustion phenomena of the pyrotechnic charge varying with pin shaft motion. In contrast, scant information is available in the literature on models that include all the parameters that govern the functional performance, and that deal with the effects of the design parameters on the performance. Therefore, the aforementioned works are not sufficient to fully understand the physics of the device.

The objective of this work is to develop an analytical model that includes all parameters that govern the function of the pin puller. This practical model is designed to aid in understanding how the pin puller functions, which design variables dominantly affect the function, and the size of the functional margin.

The outline of this paper is as follows. A mathematical model for pin puller physics is described in Sec. 2. The experiments used to derive the major performance parameters for the model are summarized in Sec. 3. The model is then verified and modified in Sec. 4 by comparing the pressure-time traces and displacements of the pin shaft for various amounts of pyrotechnic charge. In section 5, the safety factor estimation for the designed pin puller is discussed.

2. Mathematical Model

A mathematical model was developed to simulate the performance of the pin puller. Understanding of the physics

of the pin puller, such as pin shaft motion and pressure variation in the expansion chamber, is generally difficult, even if a large number of firing tests are conducted. This is because the performance variables are complexly dependent on each other. For example, burning of the pyrotechnic charge increases the pressure and temperature of the expansion chamber, which in part recursively affects its burning characteristics. This is attributed to the dependency of the burning rate on pressure and temperature. Also, the pin shaft movement similarly affects the pressure and temperature; namely, the volume of the expansion chamber is increased as the pin shaft moves, resulting in a decrease of the pressure and temperature.

Because of these difficulties, we formulated a mathematical model based on the energy conservation equation and other constitutive equations (related to force balancing and geometrical constraint), which can predict the expansion chamber pressure as well as the pin shaft displacement as functions of time. Figure 2 is a schematic of the pin puller for model calculation. In this model, several assumptions are adopted: all flow variables are uniform inside the chamber; the combustion gas behaves as an ideal gas; and only the contribution of reaction gases is considered, whereas that of the condensed phase is ignored. Also, for simplicity of calculation, the wall between the space filled by the pyrotechnic charge and the expansion chamber is not considered, although there is a metal rupture disk of the initiator. In reality, the disk ruptures when the pressure exceeds a certain level, allowing the product gases to flow into the expansion chamber.

The conservation equations for the expansion chamber are:

$$\frac{d(\rho V)}{dt} = \dot{m}_{gen} \tag{1}$$

$$\frac{d(\rho V c_v T)}{dt} = \eta_p \left(\dot{m}_{gen} c_p T\right) - \left(PA_p - W_p \cos\theta\right) v_p - \dot{Q}_{loss} \tag{2}$$

$$P = \rho R_g T \tag{3}$$

where T, C_v, and C_p are the gas temperature and specific heat capacities. The effective pin shaft area, the pin shaft velocity, and work performed by the pin shaft are expressed as A_p, V_p, and W_p, respectively.

In Eq. (2), η_p is a correction factor based on the non-ideal gas characteristics, and $\dot{Q}_{loss}$ is a parameter associated with heat transfer to the housing (see Sec. 4.1 for details). The $\dot{m}_{gen}$ is the mass flow rate generated by the burning pyrotechnic charge which can be calculated by

$$\dot{m}_{gen} = \eta_g \rho_p A_b r_b \tag{4}$$

Here, η_g is a correction factor corresponding to the fraction of gases among the reaction products (see table 1). The burning rate r_b is expressed as a function of the chamber pressure P,

$$r_b = aP^n \tag{5}$$

The area of burning surface, A_b, in Eq. (4) is a function of the burning distance *e* and can be obtained using the geometry of the loaded pyrotechnic charge. It can be expressed as $A_b = N \cdot 4\pi r^2$ by assuming that pyrotechnic granules consist of *N* spherical grains with the same *r* radius, although they consist of various granule sizes compacted into a cylindrical shape by a pressing process [7]. The value $r = 24\ \mu m$ was used in the model calculation, which is comparable to a typical $KClO_4$ crystal grain size of approximately $20 \pm 2.5\ \mu m$ (MIL-P-217 Grade A, Class 4).

The combustion products of the pyrotechnic charge are analyzed under the constant pressure condition (6.894757 MPa) using the NASA-Lewis Chemical Equilibrium Program CEA code [15], and the result is listed in Table 1. It was found that the gas weight fraction of combustion products is about 0.43. This value is incorporated as the correction factor η_g in Eq. (4). The results obtained from the CEA code including thermodynamic properties such as gas temperature, molecular weight, and specific heat ratio are also used in the model calculation.

The volume V of the expansion chamber in Eq. (2) is initially fixed, and then increased as ZPP is consumed and the pin shaft moves. This leads to a change of the chamber pressure *P*. Thus, these volume variations are included in the governing equation as

$$\frac{dV}{dt} = A_b r_b + A_p v_p \tag{6}$$

The combustion is terminated in the model calculation

Table 1. Combustion products

Reactant (state)	Combustion Product (state, mole fraction)
Zr (s) + $KClO_4$ (s) + Graphite (s) + Viton (s)	ZrO_2 (l, 0.32249) + KCl (g, 0.1869) + O (g, 0.14274) + Cl (g, 0.8003) + O_2 (g, 0.06907) + CO (g, 0.06746) + K (g, 0.05823) + ZrO_2 (g, 0.02576) + KF (g, 0.01218) + etc.

DOI:10.5139/IJASS.2014.15.1.102

when the burning distance e is equal to or greater than the radius of the spherical grains of ZPP, which is expressed by

$$\frac{de}{dt} = r_b \tag{7}$$

The pin shaft motion is governed by Newton's second law, which can be expressed as

$$\frac{dv_p}{dt} = \frac{F}{m_p} = \frac{g}{W_p}\left(F_{pr} - F_{sh} - F_{or} - F_{ld} - F_{lm}\right) \tag{8}$$

The pin shaft can move to the full stroke only if the force induced by gas pressure, F_{pr}, overcomes other resistive forces: the force needed to cut the shear pin, F_{sh}; the two frictional forces of F_{or} and F_{ld}; and the locking force of F_{lm}. The F_{sh} can be determined either by the shear test of the shear pin itself directly or by calculation using the information of the diameter and the material strength of the shear pin. Once the shear pin is cut, the pin shaft then starts to move. Hence, F_{sh} becomes zero after severing of the shear pin. Movement of the pin shaft is retarded by both F_{or} and F_{ld}. F_{or} is the friction between the chamber wall and the three O-rings fitted on the pin shaft. According to the Parker O-ring handbook [16], this frictional force is a function of pressure, and thus is employed in the model by interpolation of the graph in the handbook as follows:

$$F_{or} = 9.8\left(4.4 + 0.00232P\right) \tag{9}$$

with the unit of pressure P given in psi (pound per square inch). The latter is the friction between the pin shaft end and the bore of the object to be released (in this instance, a missile), which depends on the angle θ and the object's weight as illustrated in Fig. 2. This frictional force is modeled as follows:

$$F_{ld} = \mu N_m = \mu W_m \sin\theta \tag{10}$$

where μ is a friction coefficient that is determined from a compression test, as described in Section 3.4.

In Eq. (8), F_{lm}, generated by plastic deformation at the locking mechanism, is the force needed to hinder the pin shaft movement. The force F_{lm} varies in such a manner that it is zero from the start point to where the contact end of the moving pin shaft first meets the stud, and it is then steeply increased. This force depends on radial stresses and the contact area of the overlapped region. Calculating this force analytically is quite difficult: it includes the relatively large plastic flow of the two distinct metals due to the dimensional overlap, unknown dynamic response of the metals, and complicated contact surface changes. Due to this difficulty, the force in the model calculation is determined by the experiment described in section 3.3.

We have now established the governing equations to evaluate the pressure in the expansion chamber and the pin shaft movement. These equations must be converted into forms that are easy to handle. Through some mathematical manipulation, a set of six ordinary differential equations (ODEs) are derived as follows:

$$\frac{d\rho}{dt} = \frac{\dot{m}_{gen} - \rho_p\left(A_b r_b + A_p v_p\right)}{V} \tag{11}$$

$$\frac{dP}{dt} = \frac{\eta_p\left[\gamma R_g T_f \dot{m}_{gen} - (\gamma-1)\left(P A_p - W_p \cos\theta\right)v_p\right] - P\left(A_b r_b + A_p v_p\right) - (\gamma-1)\dot{Q}_{loss}}{V} \tag{12}$$

$$\frac{dV}{dt} = A_b r_b + A_p v_p \tag{13}$$

$$\frac{de}{dt} = r_b \tag{14}$$

$$\frac{dv_p}{dt} = \frac{g}{W_p}\left(PA_p - F_{sh} - F_{or} - F_{ld} - F_{lm}\right) \tag{15}$$

$$\frac{dl}{dt} = v_p \tag{16}$$

In Eq. (12), the second term in the numerator of the right-hand side is introduced to take into account the loss by air resistance at the front of the moving pin shaft and the weight of the pin shaft itself, and the third term is also employed for the loss due to volume increase by movement of the pin shaft. These ODEs should be solved simultaneously. The Runge-Kutta integration scheme can be used for the calculation.

3. Experiment

3.1 Mechanical Tests

In order to complete the model formulation, we need to specify some parameters that cannot be determined analytically in the previous section: F_{sh}, F_{lm}, and F_{ld}. The first two parameters are associated with classical problems of metal-cylinder shearing and interference-shaft-tube fitting, respectively [17, 18]. Although the phenomena are well known in practical applications, appropriate analytical solutions are hard to find because of the theoretical difficulty. In addition, the dynamic effects involved in this study make these problems more difficult. Very fast movement of the pin shaft creates an impact load. In this situation, solving the complex problems involving the deformation mode change, strain hardening effect, strain wave propagation, and a large metal flow would be another research topic

beyond the scope of the present study. Hence, we chose the experimental method to specify these parameters by quasi-static mechanical tests.

3.2 Shear force of the shear pin, F_{sh}

With specimens of the inert pin puller, the compression test was carried out using Instron 5582, capable of 100,000 N. The cross-head speed was set to 100 mm/min, as fast as possible, in order to simulate the shear pin that undergoes impact loading of high strain rate. The applied axial force and displacement were simultaneously recorded. Figure 3 shows the applied axial force during compression as a function of distance for five inert pin pullers.

The curves reveal a somewhat peculiar characteristic in that the load values decrease gradually after the plateaus, in contrast to the rapid drop usually seen in stress-strain curves. The average maximum load is 123 N, which is slightly higher than the shear load that can be analogized from the shear strength of 207 MPa for a heat-treated AL6061-T6 rod of 0.8 mm diameter. These results are due to the inexact shear behavior of the pin (e.g., bending effect) due to the gap between the parts for dimensional tolerance. Despite the complicated load-displacement shape shown in Fig. 3, the F_{sh} is simplified to a right triangle shape in the model. In other words, the force increases linearly to 123 N, and then becomes zero. This is because there are insignificant effects on the resistive forces because the shear force itself is relatively low.

3.3 Locking Force, F_{lm}

The locking force was measured using a compression test similar to the method used for the shear pin. Here, the locking force, a major resistive force against pin shaft movement, refers to the force absorbed by the locking mechanism. Figure 4 shows the test result with three specimens of the inert pin pullers. As the displacement increases, the force rises relatively rapidly at the beginning, and then gradually flattens out, reaching a maximum of 5,000 N. The inflection region belongs to the yield point of the materials.

The force-displacement trace in Fig. 4 was modeled by the curve fitting as follows:

$$F_{lm} = -28.47 + 186.53(1 - Exp(-l/0.095)) + 607.2(1 - Exp(-l/1.729)) \quad (17)$$

where l is the pin shaft displacement. However, there is a disparity between variables: the variable in Eq. (17) is the displacement, whereas the independent variable in Eqs. (11) ~ (16) is time. This force-displacement, however, can be incorporated into force-time in the model, as we know the displacement of the pin shaft at every time increment in solving the ODEs.

3.4 Shaft Frictional Force, F_{ld}

A frictional resistance occurs when the pin shaft retreats from the hole of the object to be released, i.e., the missile. The friction is dependent on the weight of the object and the inclined angle θ with respect to the horizontal. The static friction coefficient μ in Eq. (10) is needed to calculate the force F_{ld}. The coefficient can be estimated from the experiment as depicted in Fig. 5. A force is applied perpendicularly to the pin shaft using a special apparatus to simulate the weight of the object. Under this condition, a compression force is applied along the longitudinal axis of the pin shaft by the Instron. The first force applied is called the "applied force" and the second force applied is called the "frictional force". The frictional force increases linearly with the applied force, as shown in Fig. 6. The ratio of the frictional force to the applied force, corresponding to the proportional constant μ, is 0.379.

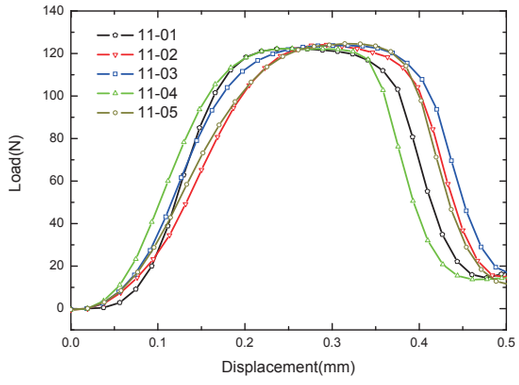

Fig. 3. Shear pin compression test results

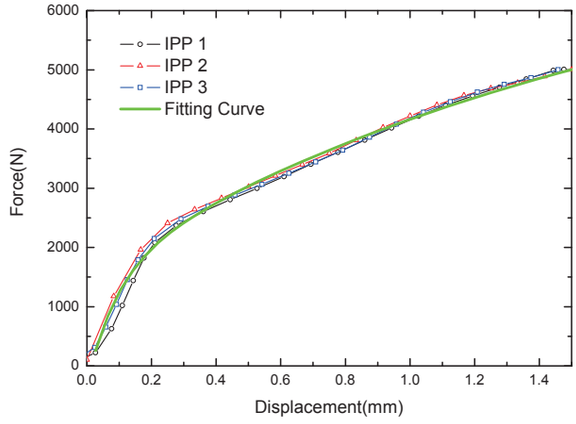

Fig. 4. Quasi-statistically measured locking force-displacement curves

DOI:10.5139/IJASS.2014.15.1.102

3.5 Firing Test

Through the model calculation, we can obtain such parameters as the gas density by combustion of the pyrotechnic charge, the pressure in the expansion chamber, and the displacement, velocity, and acceleration of the pin shaft as functions of time. Firing tests of the pin puller with different amounts of pyrotechnic charge were conducted to assess the model validity. With the test apparatus shown in Fig. 7, both the chamber pressure and pin shaft displacement were measured as functions of time. The experimental results are compared to the calculated results.

A piezo-resistive type pressure transducer (Kulite model XTL-163-190) with a sensing surface diameter of 3.7 mm was used at a sampling rate of 1 MHz. The transducer was flush-mounted on the housing of the pin puller, enabling us to acquire fast-response and accurate data [19]. For storing the data, an Agilent oscilloscope (Model Infinium 54831B) and a signal conditioning amplifier (Instrument division 2310) were used.

A DC-output potentiometer (Model LPS-30, CTA plus) was used for measuring the displacement of the pin shaft. The adaptor rod was placed between the potentiometer and the end of the pin shaft in order to make contact between them. To install the adaptor rod, a hole was drilled on the bottom of the housing as shown in Fig. 7. The sampling rate of this data was also 1 MHz.

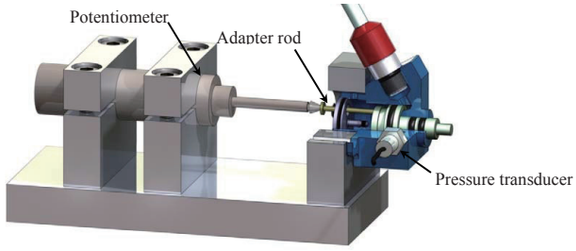

Fig. 7. Cross sectional view of the actual firing test set-up

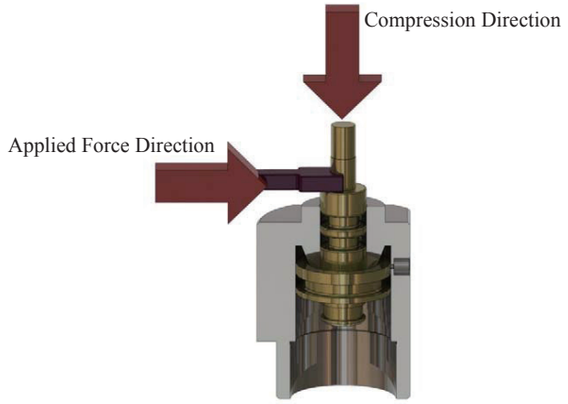

Fig. 5. Inert pin puller for measuring static frictional force

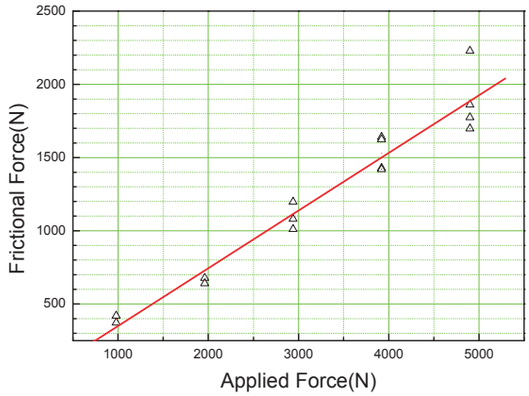

Fig. 6. Frictional force versus applied force (solid line represents a linear fit)

4. Results

4.1 Model Validation

The parameters used for model calculation are listed in table 2. Figures 8 and 9 show the time traces of pressure and displacement, respectively, for pin pullers with 53 mg of ZPP. The thin lines are for the test data and the thick lines are for the calculated data. These curves were obtained under the condition that there were no objects to be released, meaning that there is no frictional force, F_{id}. It is seen that the model yields results that are in fairly good agreement with the test data. For the best fitting of the curves, the correction factor η_p and the heat loss rate factor $\dot{Q}_{loss}$ in the model were adjusted to 0.68 and 161 J/kg s, respectively. The correction factor η_p was taken into account because of the non-ideal gas characteristics of the pyrotechnic combustion products, energy loss caused by interaction between the combustion gas and products in a condensed phase, and the rupture of the initiator's closure disk. The heat loss rate factor $\dot{Q}_{loss}$ is difficult not only to calculate theoretically but also to obtain experimentally.

The pin shaft begins to move at 0.1 ms after the pressure in the expansion chamber starts to rise, and then reaches its full stroke of 9.2 mm at about 0.7 ms. This implies that the maximum velocity of the pin shaft is about 24 m/s. As soon as the pin shaft reaches its full stroke, the pressure curve decreases with time at a minimal gradient, which is supposedly due to heat transfer to the housing.

4.2 Effect of pyrotechnic charge amounts

Additional firing tests were conducted to confirm whether the model validity is maintained for different amounts of pyrotechnic charge. In these tests, a range of 33 mg ~ 63 mg of ZPP was used in the pin puller. The test data were compared to the model calculations in terms of the pressure and the displacement versus time in Figs. 10 and 11, respectively. It can be seen that the predicted and measured results agree for both pressure and pin shaft displacement. Although several firing tests were conducted for the same amount of ZPP, only typical data is represented in the figures for simplicity.

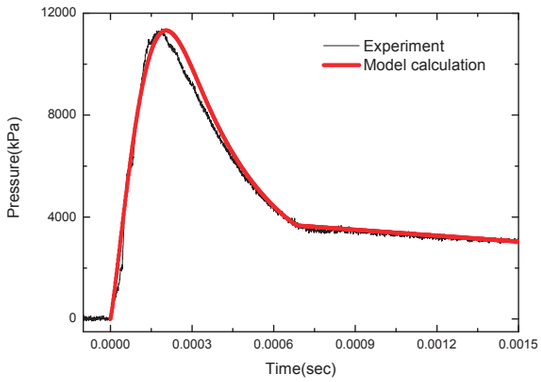

Fig. 8. Predicted and experimental pressure histories in firing test

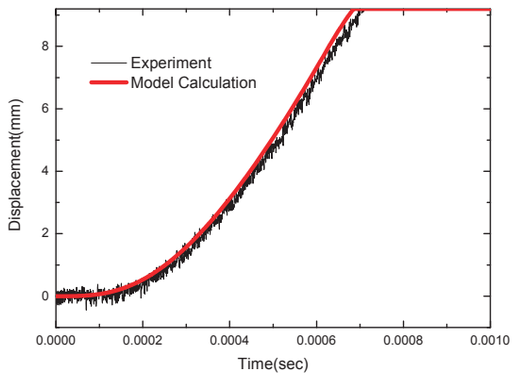

Fig. 9. Predicted and experimental pin shaft displacements in firing test

5. Discussion

Usually, failure of pyrotechnic devices causes catastrophic failures of the total system because of the vital applications required of the pyrotechnic devices. In this study, for example, failure of the pin puller may lead to mission failure of missiles since the onset of the next launch event is determined by whether the pin puller functions properly. The pin puller thus needs to have high reliability, and the evaluation of its reliability may be very important. Reliability evaluation of this type of device, however, is not easy, due to its 'one-shot' behavior. Because repeated tests are impossible, a large number of devices are thus needed to evaluate reliability with statistical significance. However, only several tens of the pin pullers are realistically available for the test. Furthermore, the tests can be performed at the final phase of the development, meaning that it is difficult to modify the design parameters. In this context of reliability, a model that can explain the physics of the pin puller is critically needed. The model we have developed can provide information on gas production by pyrotechnic combustion, pressure evolution in the expansion chamber, resistance to pin shaft motion, and dynamics such as moving displacement, velocity, or acceleration of the pin shaft, particularly in the beginning phase of development. It may be worth considering that most of this information is difficult to obtain from the firing tests. This analytical model can be applicable for probabilistic approaches, requiring much

Table 2. Parameters for model calculation

parameter	value	parameter	value
r	2.4E-5 (m)	stroke	9.2E-3 (m)
A_p	1.756E-4 (m^2)	V_{ini}	0.627E-6 (m^3)
a	0.741 (in/s)	F_{sh}	123 (N)
n	0.182	μ	0.379
T_f	4810 (K)	W_p	0.294 (N)
ρ_p	2.44E3 (kg/m^3)	γ	1.1038

DOI:10.5139/IJASS.2014.15.1.102

repeated calculation, for later reliability prediction of the pin puller.

Reliability is the possibility of the success of a system. Success of the pin puller can be defined as the pin shaft retreating to the predetermined position when fired. As stated earlier, this is possible only when the force generated by combustion of the pyrotechnic charge is capable of overcoming other resistive forces. According to a deterministic design concept, the possibility of success can therefore be simply represented as a margin of safety, which in this case is the ratio of the generated forces to the resistive forces against pin shaft movement. The pin puller functions successfully if $\frac{F_{gen}}{F_{res}} \geq 1$.

By this definition, however, representing the success possibility of the pin puller is difficult, because both F_{gen} and F_{res} vary with time. The points in time at which each force is evolved differ, and the aspects of variation for each force also differ significantly. In this instance, the definition of impulse (i.e., the product of force and time) or energy (i.e., the product of force and displacement), instead of the two forces, can be more valuable. Figure 12 shows the calculation results represented by this definition, in the case where the pin puller has 53 mg ZPP, when the weight of the missile is 115N and the launch angle is 30 degree.

From this viewpoint, success in the current work can be defined again as the ratio of the generated energy to the consumed energies: $\frac{E_{gen}}{E_{con}} \geq 1$. The generated energy E_{gen} is obtained by the integration of the force F_{pr} with respect to the displacement, whereas the consumed energy E_{con} is the sum of the relevant integration values of the four resistive forces, F_{sh}, F_{or}, F_{ld}, and F_{lm}. The magnitude of these energies is represented in Fig. 13, normalized by the generated energy.

As can be seen in Fig. 13, the largest consumption of energy, corresponding to approximately 47 percent of the generated energy, occurs in the locking mechanism to prevent rebound of the pin shaft. The next consumption is performed by the O-ring friction, which is more than five percent of the generated energy. It is interesting to note that the energy consumption by the friction between the pin shaft and the object to be released is the smallest. Consequently, the functional safety factor is approximately 1.84, which in fact is thought to be adequate [20].

The amount of pyrotechnic charge is a crucial variable that determines the possibility of success for the pin puller. However, larger amounts of pyrotechnic charge are not always better solutions, because excessive charge creates a higher pyrotechnic shock with detrimental effects. In the model calculation with 62.6 mg of ZPP, the safety factor increases to 2.19. The proper amount of pyrotechnic charge can be controlled through this model.

It is important, however, that this performance modeling approach rules out the variance of performance variables. The possibility of success should be carefully considered in

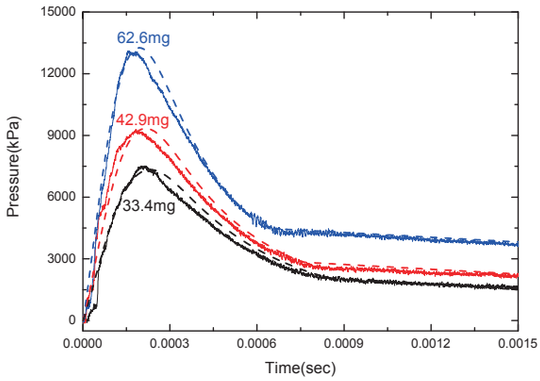

Fig. 10. Comparison of predicted (dashed line) and measured expansion chamber pressure history

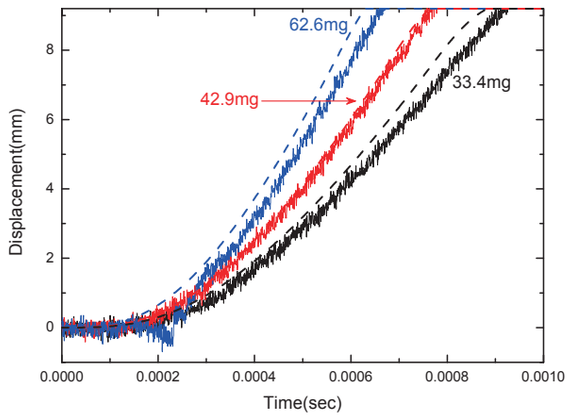

Fig. 11. Comparison of predicted (dashed line) and measured pin shaft displacement versus time

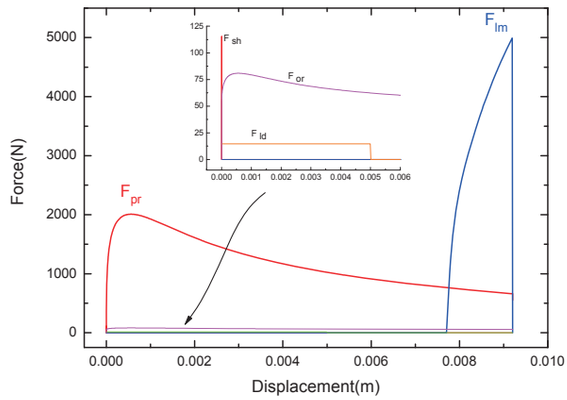

Fig. 12. Forces related to actual firing of a pin puller

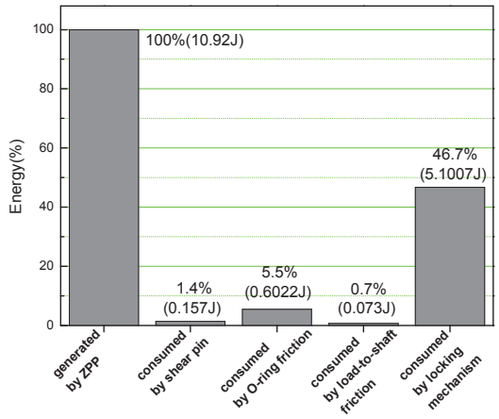

Fig. 13. Comparison of generated and consumed energy

that all the variables included in the manufacture and design have certain randomness and probabilistic fluctuations.

6. Conclusions

A model was developed to predict the performance of the pin puller. This model is based on one-dimensional gas dynamics and empirical relationships obtained from the quasi-static mechanical tests. This simple model obtains results that are in good agreement with the test data overall by adjusting correction factors. The present model makes it possible not only to understand the very complicated pin puller physics involving the pressure in the expansion chamber and the displacement of the pin shaft with time, but also to know the effects of variables on the performance. A particular strong point of the present study is that this information can be obtained from a small number of firing tests or inert tests in the beginning phases of development. Because of this advantage, the current approach can be applied to design one-shot devices used in aerospace and military applications.

References

[1] O. Brauer, *Handbook of Pyrotechnics*, Chemical Publishing Co. Inc., New York, 1974,

[2] D. J. Finney, *Probit Analysis a Statistical Treatment of the Sigmoid Response Curve*, Cambridge Univ. Press, London, 1952.

[3] J. W. Dixon, and A. M. Mood, "A Method for Obtaining and Analyzing Sensitivity data," *Journal of the American Statistical Association*, Vol. 43, No. 241, 1948, pp. 109–126.

[4] H. J. Langlie, *A Reliability Test Method for One-Shot Items*, Technical Report U-1792, Aeronutronic Division of Ford Motor Company, Newport Beach, California, 1965.

[5] Barry T. Neyer, "A D-Optimality-Based Sensitivity Test," *Technometrics*, Vol. 36, No. 1, 1994, pp. 61–70.

[6] Hobin S. Lee, "Modeling of a Hydraulically Damped Pyrotechnic Actuators", *47th AIAA Aerospace Science Meeting including the New Horizons Forum and Aerospace Exposition*, AIAA, Orland, FL, 2009, pp. 761.

[7] Adam M. Braud, Keith A. Gonthier, and Michele E. Decroix, "System Modeling of Explosively Actuated Valves", *Journal of Propulsion and Power*, Vol. 23, No. 5, 2007, pp.1080-1095.

[8] S. B. Shmuel, "Performance Analysis of a Normally Closed Pyrovalve", *46th AIAA/ASME/SAE/ASEE Joint Propulsion Conference and Exhibition*, AIAA, Indianapolis, IN, 2002, pp. 3552.

[9] J. D. Kutschka, "Pyrotechnically Actuated Mechanism Performance Prediction and Test Correlation", *36th AIAA/ASME/SAE/ASEE Joint Propulsion Conference and Exhibition*, AIAA, Huntsville, AL, 2000, pp. 3513.

[10] P. G. Amand, and J. A. Tiemon, "Mathematical Model of the Ballistic and Mechanical Behavior of Ordnance Systems", *31st AIAA/ASME/SAE/ASEE Joint Propulsion Conference and Exhibition*, AIAA, San Diego, CA, 1995, pp. 2853.

[11] K. A. Gonthier, and J. M. Powers, "Formulation, Prediction, and Sensitivity Analysis of a Pyrotechnically Actuated Pin Puller Model", *Journal of Propulsion and Power*, Vol. 10, No. 4, 1994, pp. 501-507.

[12] C. A. LaJeunesse, and M. F. Hardwick, "Design Methodology and Testing of an Electro-Explosive Valve", *Proceedings of the 1994 ASME Pressure Vessels and Piping Conference*, Honolulu, HI, 1994.

[13] J. H. Kuo, and S. Goldstein, "Dynamic Analysis of NASA Standard Initiator Deriven Pin Puller", *29th AIAA/ASME/SAE/ASEE Joint Propulsion Conference and Exhibition*, AIAA, Monterey, CA, 1993, pp. 2066.

[14] Hobin S. Lee, "Unsteady Gas-dynamics Effects in Pyrotechnic Actuators," *Journal of Spacecraft and Rockets*, Vol. 41, No. 5, 2004, pp.877-886.

[15] Bonnie J. McBride, and Sanford Gordon, "Computer Program for Calculation of Complex Chemical Equilibrium Compositions and Applications", NASA Reference Publication 1311, Part II, 1996.

[16] *Parker O-Ring Handbook 2001 Edition*, Parker Hannifin Corporation, Cleveland, OH, 2001.

[17] N. Baldanzini, "A General Formulation for Designing Interface-fit Joints with Elastic-Plastic Components", *Journal of Mechanical Design*, Vol. 126, Issue 4, 2004, pp.737-743.

[18] B. Parsons, and E.A. Wilson, "A Method for Determining the Surface Contact Stresses resulting from

Interference Fits", *Journal of manufacturing Science and Engineering*, Vol. 92, No. 1, 1970, pp.208-218.

[19] Adreas Dibbern et al., "Implication of Dynamic Pressure Transducer Mounting Variations on Measurements in Pyrotechnic Test Apparatus", *45th AIAA/ASME/SAE/ASEE Joint Propulsion Conference & Exhibit*, AIAA, Denver, Colorado, 2009, pp. 4992.

[20] "Criteria for Explosive Systems and Devices on Space and Launch Vehicles", *AIAA S-113-2005 Standard, American Institute of Aeronautics and Astronautics*, AIAA, Reston, VA, 2005, p.16.

Acknowledgments

The authors gratefully acknowledge both In-sik Kim and Gook-hyun Baek of the Agency for Defense Development, Daejeon, for the many useful discussions on the actual test related to the pressure transducer mounting technique and combustion gas product characteristics of ZPP, respectively. The authors also thank Mi-ra Kwon and Ja-ho Jung of the Hanwha Corp. R&D Center, Daejeon, for manufacturing the device and for their technical collaboration on all experiments.

Symbols and Abbreviations

A_b	Burning surface area (m^2)
A_p	Effective Pin shaft area (m^2)
a	Burning-rate slope coefficient ($m/s/Pa^n$)
c_p	Specific heat capacity (J/kg K)
c_v	Specific heat capacity (J/kilomole K)
e	Burning distance of pyrotechnic charge column (m)
F	Force (kg m/s^2)
g	Gravitational acceleration (9.8 m/s^2)
l	Pin shaft displacement (m)
$\dot{m}_{gen}$	Mass generation rate (kg/s)
m_p	Mass of pin shaft (kg)
N	Number of ZPP grains
N_m	Normal force (N)
n	Burning-rate power constant
P	Chamber pressure (Pa)
$\dot{Q}_{loss}$	Heat transfer rate (J/s)
R_g	Universal gas constant (8.3143×10^3 J/kilomole K)
r	Radius of ZPP grain (m)
r_b	Burning rate (m/s)
T	Temperature (K)
T_f	Gas flame temperature (K)
t	Time (s)
V	Volume (m^3)
V_o	Initial volume of expansion chamber (m^3)
v_p	Pin shaft velocity (m/s)
W_m	Load weight (N)
W_p	Work done by pin shaft (N)

Greek Symbols

γ	Ratio of specific heats
θ	Angle (Rad)
η_g	Gas fraction of the combustion products (0.43)
η_p	Correction factor
μ	Friction coefficient
ρ	Density (kg/m^3)
ρ_p	Pyrotechnic charge density (kg/m^3)

Subscripts

b	burning
con	consumed
g	gas
gen	generated
ini	initial
ld	load
lm	locking mechanism
or	O-ring
pr	pressure
res	resistive
sh	shear